



HAL
open science

Stochastic modelling of turbulent flows for numerical simulations

Carlo Cintolesi, Etienne Mémin

► **To cite this version:**

Carlo Cintolesi, Etienne Mémin. Stochastic modelling of turbulent flows for numerical simulations. 2019. hal-02044809

HAL Id: hal-02044809

<https://hal.science/hal-02044809>

Preprint submitted on 21 Feb 2019

HAL is a multi-disciplinary open access archive for the deposit and dissemination of scientific research documents, whether they are published or not. The documents may come from teaching and research institutions in France or abroad, or from public or private research centers.

L'archive ouverte pluridisciplinaire **HAL**, est destinée au dépôt et à la diffusion de documents scientifiques de niveau recherche, publiés ou non, émanant des établissements d'enseignement et de recherche français ou étrangers, des laboratoires publics ou privés.

Stochastic modelling of turbulent flows for numerical simulations

Carlo Cintolesi · Etienne Mémin

Received: date / Accepted: date

Abstract The stochastic model proposed by Mémin [24] for turbulent flow simulations is analysed, both theoretically and numerically. It is shown to be a generalisation of the classical large-eddy simulation approach, and to describe a richer physics. The model does not lead to the eddy-viscosity assumption and can be reduced to Smagorisky model under restrictive hypotheses; hence, it can be considered as a generalisation of classical models. Simulations of a turbulent channel flow at $Re_\tau = 590$ shows the presence of physical phenomena usually not reproduced; namely a weak turbophoresis and of a turbulent compressibility linked to streaks structures. The turbulent kinetic energy budget suggests that the model is more effective in dissipating energy near the wall. For the sake of completeness, alternative and detailed derivation of the stochastic model is reported in detail in the appendix.

Keywords Stochastic models · Turbulence modelling · Numerical simulations · OpenFOAM.

1 Introduction

The reliable numerical simulation of turbulent flows is still nowadays a challenging issue, both in terms of mathematical modelling and of computational cost required. In the last decades, different techniques were developed to tackle this problem, the most fruitful for practical applications being the Reynolds-averaged simulation and the Large-Eddy Simulation (LES) methodologies. Despite the continuous improvements with increasing accuracy of the models,

C. Cintolesi
INRIA Rennes, Fluminance group, Campus de Beaulieu, F-35042 Rennes (France)
E-mail: carlo.cintolesi@gmail.com

E. Mémin
INRIA Rennes, Fluminance group, Campus de Beaulieu, F-35042 Rennes (France)
E-mail: etienne.memin@inria.fr

22 such methodologies are developed within a deterministic framework. Hence,
23 they cannot completely represent the random nature exhibited by turbulent
24 flows, that eventually requires the use of stochastic calculus. In the field of
25 geophysical flows, probabilistic models are used to correct the effects of the
26 coarse spatial discretisation. Similarly, the stochastic variables can be em-
27 ployed to account for the unresolved processes in the numerical reproduction
28 of engineering and environmental flows.

29 The literature proposes different approaches on this topic. The stochastic
30 Langevin equation is derived assuming that a fluid-particle velocity is per-
31 turbed by a Brownian motion, which is found to well described the dynamics
32 of turbulent flows; see Pope [35]. This equation was used in the framework
33 of Probability Density Function (POF) methods to reproduce homogeneous
34 isotropic turbulence, but also inhomogeneous and anisotropic turbulence by
35 Pope [36] and by Durbin & Speziale [8], respectively. Orszag [33] and Leslie [22]
36 introduced the Eddy-Damped Quasi-Normal Markovian (EDQNM) models;
37 see the overview by Lesieur [21]. The large-scale equations were closed in
38 spectral space through a Gaussian closure. They were particularly suitable
39 to study strong non-linearity in the small-scale turbulence. In the same frame-
40 work, Chasnov [5] develops a forced-dissipative model, where the large-eddy
41 Navier-Stokes equations were corrected by a stochastic force terms. This was
42 a Gaussian forcing uncorrelated in time, homogeneous and isotropic in space.
43 Kraichnan [16] exploits a different approach: the momentum equations are
44 replaced by a set of equations with same mathematical properties, which are
45 closed using a Gaussian stochastic model. This theory leads to valuable results
46 in terms of mathematical properties (existence, singularities) and physical ef-
47 fects (turbulent diffusion, backscatter) analyses. Frederiksen [11] shows that
48 the same strategy can be used for a stochastic modelling of barotropic flows
49 or in quasi-geostrophic approximation, that includes the interaction between
50 topography and small-scale eddies. The randomness effects can be also explic-
51 itly introduced by means of *ad hoc* stochastic terms. Investigating the plane
52 shear mixing layer, Leith [20] improves the accuracy of LES with Smagorinsky
53 model by introducing an explicit stochastic terms. On the theoretical side,
54 Flandoli [9] studied fluid dynamic systems corrected with a random white
55 noise force to reproduce the complex phenomena related to turbulence.

56 These attempts have some limitations: the POF and EDQNM models re-
57 quired to work in the spectral space instead of the physical one; there is a
58 certain degree of arbitrariness when explicit random terms are introduced
59 (e.g. the random forcing should be multiplicative or additive); and overall the
60 models can be hardly generalised for practical applications.

61 The methodology here presented aims to overcome these shortcomings. It
62 develops from a different starting point: the fluid-particle trajectory in the
63 Lagrangian framework is assumed to be a random process. It is expressed
64 by a semimartingale, where the finite-variation part represents the smooth
65 macroscopic velocity, while the martingale models the perturbations due to
66 the turbulent motion. Consistently, an expression of the velocity is found and
67 stochastic calculus is used to derived the stochastic equations of motions. In

68 such a procedure, the use of the Itô-Wentzell formula is crucial to compute the
69 time derivative, see Kunita [18]. A first work in this direction was that one of
70 Brzeźniak [2], subsequently extended by Mikulevicius and Rozovskii [27] and
71 Flandoli [10]. Globally, these works focused on the mathematical properties of
72 the stochastic equations. The work of Mémin [24] follows a similar approach
73 and developed the so called model under Location Uncertainty (LU), which
74 is oriented to practical application in computational fluid dynamics. Recently,
75 Holm [13] derived a similar set of equations using Lagrangian mechanics, which
76 leads to additional terms, while Neves *et al.* [29] studied theoretically a simi-
77 lar system of equations. The LU model was applied to different applications:
78 Resseguier *et al.* [37,38,39] used it for geophysical flows simulations, where
79 it exhibits a high accuracy in reproducing extreme events and provided new
80 analysis tools. Chapron *et al.* [4] investigated the Lorentz-63 case and found
81 that LU is able to explore the region of the deterministic attractor faster than
82 the classical models. Resseguier *et al.* [40] employed it in conjunction with the
83 proper orthogonal decomposition technique for the numerical simulation of a
84 flow past a circular cylinder at $Re = 3900$.

85 Although this is a promising methodology, the inherent mathematical comple-
86 xity of stochastic partial differential equations poses some difficulties: the
87 resolution of stochastic partial equations is not straightforward and can con-
88 siderably increase the simulation time. For these reasons, Mémin [24] also
89 introduces a simplified model, where the resolution of stochastic equations is
90 avoided by modelling the effects of the random velocity term by physical as-
91 sumption. This give rise to the so called *pseudo-stochastic simulation* (PSS)
92 methodology: the flow dynamics is described by classical partial differential
93 equations, which includes additional terms provided by the stochastic mod-
94 eling. The PSS was adopted by Harouna and Mémin [12] to investigate the
95 Green-Taylor vortex flow applying several models for the stochastic contribu-
96 tion. Chandramouli *et al.* [3] employed it to simulate the transitional wake
97 flow with coarse mesh resolution, proving that it generates a more accurate
98 outcomes with respect to classical LES.

99 Notwithstanding the above mentioned studies, a pointwise analysis of the
100 pseudo-stochastic model is lacking. The aims of the present work is to study
101 in details the characteristics of the LU and the PSS model, both theoretically
102 and numerically, establishing a parallelism with the classical LES methodol-
103 ogy. First, a theoretical analysis of the PSS equations is reported; second, a
104 simplified closure model is adopted to perform numerical simulations on the
105 plane channel flow at $Re_\tau = 590$. The simulation outcomes are discussed in
106 light of the previous theoretical analysis and the peculiarity of the PSS are
107 highlighted. The main novelty of this work is to propose a detailed and sys-
108 tematic comparison between PSS and LES approach, pointing out the physical
109 meaning of the extra term arising from the stochastic derivations (supported
110 by simulations). Moreover, after few years from its first formulation, an alter-
111 native mathematical derivation of the LU and PSS model is proposed in the
112 appendix. Efforts have been made to simplify and give a linear structure to
113 the procedure, highlighting the key hypotheses.

114 The paper is organized as follows: section 2 presents the pseudo-stochastic
 115 model and the relative turbulent kinetic budget; section 3 reports a physical in-
 116 terpretation of the model and make a comparison with the LES methodology;
 117 section 4 describe the closure model for PSS; section 5 discusses the numer-
 118 ical simulation results; section 6 gives some final remarks. In appendix A an
 119 alternative and detailed derivation of the stochastic model for turbulent flows
 120 is presented.

121 2 Pseudo-Stochastic Model

122 In this section, the stochastic formalism and the pseudo-stochastic equations
 123 are reported.

124 2.1 Stochastic formalism

125 The particle trajectory in a turbulent regime is not completely known be-
 126 cause it is subject to some random (turbulent) effects. Consequently, the fluid-
 127 particle displacement is described by the stochastic differential equations of the
 128 type:

$$129 \quad dX_t^i(x_0) = w_i(X_t, t)dt + d\eta_t^i(X_t), \quad (1)$$

130 where the index $i = 1, 2, 3$ indicates respectively the x, y, z -component in space
 131 (they are placed at top or bottom indifferently); $X_t^i(x_0)$ is the trajectory fol-
 132 lowed by a fluid-particle initially located in x_0 ; w_i is a differentiable function of
 133 bounded variation (i.e. equivalent to a deterministic function) that corresponds
 134 to the resolved flow velocity; $\eta_t^i = \int_0^t d\eta_t^i$ is a martingale that accounts for the
 135 stochastic contributions to the motion. The Einstein summation convention
 136 over repeated indexes is adopted. The stochastic contribution is constructed
 137 as a combination of a cylindrical Wiener processes $B_t^k(x)$ not differentiable in
 138 time, and a differentiable *diffusion tensor* σ_{ik} which acts as an integral kernel:
 139

$$140 \quad d\eta_t^i(x) = \int_{\Omega} \sigma_{ik}(x, y, t) dB_t^k(y) dy. \quad (2)$$

141 Notice that the stochastic processes η_t^i are uncorrelated in time and correlated
 142 in space by means of the diffusion tensor.

143 The expression of the velocity field U_i in Eulerian coordinate x is derived
 144 from equation (1); it reads:

$$145 \quad U_i(x, t) = w_i(x, t) + \dot{\eta}_t^i(x), \quad (3)$$

146 where the second term on the right-hand side expresses the stochastic velocity
 147 defined by formula (22). From a physical point of view, w_i is the velocity
 148 expected value and $\dot{\eta}_t^i(x)$ represents a noise: a generalised stochastic process
 149 that has to be defined in the space of temperate distribution, see Øksendal [31].

150 The quadratic variation of the diffusion tensor is a quantity of particular
 151 interest; it represents the time-variation of the spatial variance of the stochastic
 152 increments along time. It is named *variance tensor* and is defined as:

$$153 \quad a_{ij}(x, t) = \int_{\Omega} \sigma_{ik}(x, y, t) \sigma_{jk}(x, y, t) dy. \quad (4)$$

154 As a function, it is assumed to have all the regularity (differentiable and inte-
 155 grable in time and space) required by computation; as a tensor, it is a point-
 156 wise symmetric and semi-positive definite matrix.

157 2.2 Pseudo-stochastic equations of motion

158 The stochastic fluid dynamics equations for a Newtonian incompressible fluid
 159 are derived in appendix A. The final system (63) is composed by one set of
 160 stochastic equations and one of pure deterministic ones. The former allows
 161 to find an expression for the variance tensor a_{ij} , which is required for the
 162 resolution of the latter. Together, they provide a close system of equations
 163 that composes the LU model. Let us not that full stochastic model can be
 164 obtained by relaxing the assumption of bounded variation for the resolved
 165 velocity (see [37]).

166 In order to simplify the model by avoiding the resolution of stochastic par-
 167 tial differential equations, the variance tensor a_{ij} is not computed but modelled
 168 through physical assumptions. This choice gives rise to a hybrid model where
 169 the stochastic contribution on the governing equations is modelled by a de-
 170 terministic function, and, overall, no stochastic equations have to be resolved.
 171 Such model leads to pseudo-stochastic simulation approach. The PSS momen-
 172 tum and continuity equations for incompressible flows reads, respectively:

$$173 \quad \begin{cases} \frac{\partial w_i}{\partial t} + w_j^* \frac{\partial w_i}{\partial x_j} = -\frac{\partial p}{\partial x_i} + \nu \frac{\partial^2 w_i}{\partial x_j \partial x_j} + \frac{1}{2} \frac{\partial}{\partial x_j} \left(a_{jk} \frac{\partial w_i}{\partial x_k} \right) \\ \frac{\partial w_i^*}{\partial x_i} = 0. \end{cases} \quad (5)$$

174 where ν is the molecular viscosity, the modified pressure $p = p_h + \frac{\nu}{3} \frac{\partial w_\ell}{\partial x_\ell}$ is the
 175 sum of the hydrostatic pressure and the divergence of the velocity field (which
 176 is not solenoidal), and the effective advection velocity w_i^* reads:

$$177 \quad w_i^* = w_i - \frac{1}{2} \frac{\partial}{\partial x_k} a_{ik}. \quad (6)$$

178 The terms depending on a_{ij} account for the effects of the Stochastic Unresolved
 179 Scales (SUS) of motion, since the variance tensor is a measure of the intensity
 180 and the anisotropy of turbulent random velocities.

181 Notice that system (5) reduces to the classical Navier-Stokes equations
 182 when the a_{ij} is the zero matrix, i.e. when the stochastic contributions disap-
 183 pear.

184 2.3 Resolved kinetic energy budget

185 The turbulent kinetic energy (TKE) budget of the resolved scales of motion
 186 is presented. The resolved velocity is decomposed in a mean and a fluctuating
 187 part, respectively:

$$188 \quad w_i = W_i + w'_i, \quad (7)$$

where the capitol letter indicates the averaged field, $W_i = \langle w_i \rangle$. Variance tensor and pressure are decomposed in a similar way: $a_{ij} = A_{ij} + a'_{ij}$ and $p = P + p'$. The (resolved) turbulent kinetic energy $\kappa = w'_i w'_i / 2$ budget reads:

$$\begin{aligned} & \frac{\partial \langle \kappa \rangle}{\partial t} + \underbrace{\left(W_j - \frac{\partial A_{jk}}{\partial x_k} \frac{1}{2} \right) \frac{\partial \langle \kappa \rangle}{\partial x_j} + \left\langle \left(w'_j - \frac{\partial a'_{jk}}{\partial x_k} \frac{1}{2} \right) \frac{\partial \kappa}{\partial x_j} \right\rangle}_{\text{advection}} = \\ & = \frac{\partial}{\partial x_j} \underbrace{\left[-\langle p' w'_j \rangle + \left(\nu \delta_{jk} + \frac{A_{jk}}{2} \right) \frac{\partial \langle \kappa \rangle}{\partial x_j} + \left\langle \frac{a'_{jk}}{2} \frac{\partial \kappa}{\partial x_j} \right\rangle + \left\langle \frac{a'_{jk} w'_i}{2} \frac{\partial W_i}{\partial x_k} \right\rangle \right]}_{\text{transport}} \\ & + \underbrace{\left\langle \frac{p'}{2} \frac{\partial^2 a'_{jk}}{\partial x_j \partial x_k} \right\rangle}_{\text{turb. compress.}} - \underbrace{\left(\nu \delta_{jk} + \frac{A_{jk}}{2} \right) \left\langle \frac{\partial w'_i}{\partial x_j} \frac{\partial w'_i}{\partial x_k} \right\rangle - \left\langle \frac{a'_{jk}}{2} \frac{\partial w'_i}{\partial x_j} \frac{\partial w'_i}{\partial x_k} \right\rangle}_{\text{dissipation}} \\ & - \underbrace{\left\langle \left(w'_j - \frac{\partial a'_{jk}}{\partial x_k} \frac{1}{2} \right) w'_i \right\rangle \frac{\partial W_i}{\partial x_j}}_{\text{production}} - \underbrace{\left\langle \frac{a'_{jk}}{2} \frac{\partial w'_i}{\partial x_j} \right\rangle \frac{\partial W_i}{\partial x_k}}_{\text{loss to SUS}} \quad (8) \end{aligned}$$

189 The TKE terms are interpreted in light of the classical budget analysis, e.g.
 190 see Kundu and Cohen [17]. On the left-hand side, the second and third terms
 191 represent the TKE advection by mean and SUS effective advection velocity.
 192 On the right-hand side:

- 193 – first four terms: transport by pressure, molecular viscosity and turbulent stresses;
- 194 – fifth term: turbulent compression/expansion due to SUS;
- 195 – sixth and seventh terms: dissipation by molecular viscosity (it can be proven that A_{ij} is positive defined), resolved turbulence and SUS motions;
- 196 – eighth term: shear production, this term appears in the mean kinetic budget (not shown here) with opposite sign;
- 197 – last term: loss due to SUS also present in the mean kinetic energy budget.

201 The pseudo-stochastic TKE budget reduces to the classical one if the stochastic contribution is negligible $a_{ij} \simeq 0$. It is worth to notice that the production term includes the contribution of the fluctuations of turbulent advection velocity, while the variance tensor plays a role of a turbulent viscosity dissipation tensor.

3 Analysis of pseudo-stochastic model

The expression of fluid-particle displacement (1) states that a particle trajectory is driven by two actors: a differentiable drift velocity and a Brownian process highly fluctuating in time. In the framework of PSS, the drift velocity w_i that can be interpreted as the resolved velocity field, while the random field assembles the residual motion that are fast oscillating stochastic components, possibly anisotropic and non-homogeneous in space.

3.1 Physical interpretation

Recalling the decomposition of the velocity gradient in symmetric and antisymmetric parts, respectively called the strain-rate tensor and the rotation-rate tensor:

$$\frac{\partial w_i}{\partial x_j} = \frac{1}{2} \left(\frac{\partial w_i}{\partial x_j} + \frac{\partial w_j}{\partial x_i} \right) + \frac{1}{2} \left(\frac{\partial w_i}{\partial x_j} - \frac{\partial w_j}{\partial x_i} \right) = S_{ij} + \Omega_{ij}, \quad (9)$$

the pseudo-stochastic Navier-Stokes equation (5) and continuity equation (6) are rearranged as, respectively:

$$\begin{aligned} \frac{\partial w_i}{\partial t} + \underbrace{\left(w_j - \frac{1}{2} \frac{\partial a_{jk}}{\partial x_k} \right)}_{\text{effective advection}} \frac{\partial w_i}{\partial x_j} = & - \frac{\partial}{\partial x_i} \underbrace{\left(p_h + \frac{\nu}{3} \frac{\partial^2 a_{sk}}{\partial x_k \partial x_s} \right)}_{\text{modified pressure}} + 2\nu \frac{\partial S_{ij}}{\partial x_j} \\ & + \underbrace{\frac{1}{2} \frac{\partial}{\partial x_s} (a_{sk} S_{ki}) - \frac{1}{2} \frac{\partial}{\partial x_s} (a_{sk} \Omega_{ki})}_{\text{diffusion due to SUS}}, \quad (10) \end{aligned}$$

and

$$\frac{\partial w_i}{\partial x_i} = \underbrace{\frac{1}{2} \frac{\partial^2 a_{jk}}{\partial x_j \partial x_k}}_{\text{turb. compr.}}. \quad (11)$$

The terms that depend on variance tensor account for the influence of the SUS on the resolved scales. A physical interpretation of such terms is proposed:

Effective advection: the advection velocity is corrected by an inhomogeneous turbulence contribution. It corresponds to a velocity induced by the unresolved turbulent motions, that can be linked to the *turbophoresis* phenomenon detectable in geophysical flows; i.e. the tendency of fluid-particle to migrate in the direction of less energetic turbulence (see also [37]).

Modified pressure: the non-solenoidal velocity field leads to the presence of an isotropic turbulent factor, that has the dimension of a pressure: $p_t = \frac{\nu}{3} \frac{\partial^2 a_{sk}}{\partial x_k \partial x_s}$. This term does not contribute to the flow and it is included in the pressure gradient in the same manner as the isotropic residual stress in the Smagorinsky model, see [35].

Diffusion due to SUS: they account for the turbulent diffusion; the variance tensor plays the role of a diffusion tensor similar to a generalised eddy-viscosity matrix. Both the deformation rate and rotation-rate contribute to diffusion, unlike to the classical eddy-viscosity model in which fluid rotation-rate is assumed to be irrelevant in turbulent modelling (see also following section 3.2).

Turbulent compressibility: the continuity equation (11) suggests that the flow is turbulent-compressible; i.e. the unresolved turbulence induces a local fluid compression or expansion.

The variance tensor is the key parameter of the pseudo-stochastic model. It has the physical dimension of a dynamic viscosity [m^2/s] and carries information on the intensity and the anisotropy of the SUS. As already mentioned, a_{ij} can be interpreted as a generalised eddy-viscosity parameter. Implicitly, this leads to the hypothesis that the SUS influences the resolved flow as an alteration of fluid viscosity, that is an empirical consideration largely accepted. The divergence of the variance tensor is hereafter named *turbulent advection velocity*:

$$u_{\text{TA},i} = -\frac{1}{2} \frac{\partial a_{ij}}{\partial x_j}, \quad (12)$$

while the divergence of the turbulent advection velocity measured the *turbulent compressibility*:

$$\Phi_{\text{TC}} = \frac{1}{2} \frac{\partial^2 a_{ij}}{\partial x_i \partial x_j}, \quad (13)$$

and it is directly proportional to the isotropic turbulent factor p_t appearing in the modified pressure. The numerical simulations reported later allow to gain additional insights regarding these two quantities, we refer to section 5.3 for the numerical analysis.

3.2 Comparison with LES eddy-viscosity models

The LES methodology consists in applying a spatial filter to velocity field, and then directly resolve the filtered velocity and model the sub-filter velocities. See Sagaut [42] and Piomelli [34] for an extended introduction on this subject. Practically, the computational grid acts as an implicit spatial filter on the governing equations, which generates an extra term τ_{ij} in the classical Navier-Stokes equations:

$$\begin{cases} \frac{\partial \bar{u}_i}{\partial t} + \bar{u}_j \frac{\partial \bar{u}_i}{\partial x_j} = -\frac{\partial \bar{p}}{\partial x_i} + \nu \frac{\partial^2 \bar{u}_i}{\partial x_j \partial x_j} - \frac{\partial \tau_{ij}}{\partial x_j}, \\ \frac{\partial \bar{u}_i}{\partial x_i} = 0, \end{cases} \quad (14)$$

where the sub-grid scale (SGS) tensor is $\tau_{ij} = \overline{u_i u_j} - \bar{u}_i \bar{u}_j$, and the straight over-bar denotes the spatial filter associated to the local cell width, computed as $\bar{\Delta} = (\Delta x \Delta y \Delta z)^{1/3}$. Adopting the eddy-viscosity assumption, the

267 anisotropic part of such tensor reads:

$$268 \quad \tau_{ij}^R = \tau_{ij} - \frac{\tau_{kk}}{3} \delta_{ij} = -2\nu_{\text{SGS}} \bar{S}_{ij}, \quad (15)$$

269 where ν_{SGS} is the SGS viscosity parameter, which has to be specified by additional models (e.g. Smagorinsky model, Spalart-Allmaras, $k - \omega$, $k - \epsilon$). Equation (15) implies that: (a) the anisotropic Reynolds stress tensor is aligned with the mean strain-rate tensor; (b) the two are directly proportional through a single parameter, equal for all the six independent components of τ_{ij}^R .

274 The pseudo-stochastic model is equivalent to a constant eddy-viscosity model if the variance tensor is expressed by $a_{ij} = 2\nu_{\text{SUS}} \delta_{ij}$ where the SUS viscosity ν_{SUS} is constant. In this sense, the pseudo-stochastic model can be considered a generalisation of the eddy-viscosity model. The theoretical advantages of the former to the latter are pointed out:

- 279 1. The PSS does not rely on hypothesis (a). The effects of unresolved scales of motion are given by a_{ij} , without imposing any constraints on the directions along with the SUS acts on the resolved flow.
- 280 2. The PSS does not rely on hypothesis (b). The tensorial form of a_{ij} allows to reproduce the anisotropy of unresolved turbulence, i.e. different turbulent contributions along different directions.
- 281 282 3. The extra terms in PSS account for turbulent effects usually not considered in the classical models, namely turbulent advection and turbulent compressibility.
- 283 284 285 286 287

288 The eddy-viscosity models are quite reasonable for simple shear flows and it is largely applied in computational fluid dynamics. However, most of their shortcomings derive from the fact that hypotheses (a) and (b) are not generally satisfied; see Pope [35]. Efforts have been made to develop alternative models where the principal axis of τ_{ij}^R are not forced to be aligned with those of the mean strain tensor (e.g. the Reynolds-stress models), or where equation (15) is substituted by a non-linear viscosity models, in which the rotation strain-rate comes into play, see for example Bauer *et al.* [1]. In geophysical flow simulations, the strong grid anisotropy between horizontal and vertical directions is successfully handled using a directional eddy-viscosity, see Roman and Armenio [41].

299 It is worth mentioning that the eddy-viscosity parameter a_{ij} comes directly from the basic assumption of velocity decomposition in a smooth and a fast oscillating components (3), whereas it is introduced in LES equations through an *ad hoc* physical assumption.

303 4 Variance tensor model

304 In the LES framework, a popular model for ν_{SGS} in LES methodology is the the Smagorinsky model, first proposed by Smagorinsky [43] for simulation of environmental flows (see also Deardorff [7]). It is derived under the hypothesis

307 of local equilibrium between production and dissipation of turbulent kinetic
308 energy, and reads:

$$309 \quad \nu_{\text{SGS}} = c_s^2 \Delta^2 |\bar{S}|, \quad (16)$$

310 where $|\bar{S}|$ is the norm of the strain-rate tensor. The parameter c_s^2 is set con-
311 stant and can be evaluated from experiments, direct numerical simulations or
312 analytical considerations, e.g. see Lilly [23].

313 In order to perform a close comparison with the LES methodology, the
314 variance tensor is modelled by a simple model analogous to the Smagorinsky
315 model:

$$316 \quad a_{ij} = c_m \Delta^2 |\bar{S}| \delta_{ij} \quad (17)$$

317 where Δ is the cell grid width and c_m is a model parameter. Hence, the variance
318 tensor reduces to a diagonal matrix with equal elements because turbulence is
319 assumed isotropic and homogeneous in all directions.

The relation with the classical Smagorinsky model is now highlighted. In
LES, having applied the Smagorinsky model, the anisotropic Reynolds stress
tensor reads:

$$-\frac{\partial \tau_{ij}^R}{\partial x_i} = \frac{\partial}{\partial x_i} (2c_s^2 \Delta^2 |\bar{S}| S_{ij}) = S_{ij} \frac{\partial C_s |\bar{S}|}{\partial x_i} + \frac{C_s}{2} |\bar{S}| \frac{\partial^2 w_j}{\partial x_i \partial x_i}, \quad (18)$$

where $C_s = 2c_s^2 \Delta^2$ denotes an auxiliary variable, c_s^2 is the Smagorinsky param-
eter and the velocity is divergence-free. In the PSS, the total turbulent model
can be expressed by a single term, that gathers the dissipative and turbulent
advective contributions. Applying formula (17) with $c_m = 2c_s^2$ and defining
 $C_m = c_m \Delta^2$, such a term becomes:

$$\frac{1}{2} \frac{\partial^2 a_{sk} w_i}{\partial x_s \partial x_k} = \underbrace{\left(S_{ij} \frac{\partial C_m |\bar{S}|}{\partial x_i} + \frac{C_m}{2} |\bar{S}| \frac{\partial^2 w_j}{\partial x_i \partial x_i} \right)}_{\text{eddy-viscosity terms}} + \underbrace{\Omega_{ij} \frac{\partial C_m |\bar{S}|}{\partial x_j}}_{\text{rotational term}} + \underbrace{\frac{w_i}{2} \frac{\partial^2 C_m |\bar{S}|}{\partial x_j \partial x_j}}_{\text{strain-rate diff.}}, \quad (19)$$

320 where the first two terms on the right-hand side have (formally) the same ex-
321 pression as (18), while the third and fourth term are additional contributions.

322 The PSS with isotropic constant model reduces to the LES Smagorinsky
323 model under two approximations:

- 324 1. the rotation-rate does not contribute to turbulence effects on the mean
325 flow, thus it is neglected;
- 326 2. the norm of strain-rate tensor is almost harmonic (Laplacian is close to
327 zero), which makes the fourth term negligible.

328 Notice that the latter hypothesis implies that the continuity equation (6) turns
329 into the classical solenoidal constrain. Therefore, the LES Smagorinsky model
330 can be interpreted as a particular case of the PSS constant isotropic model.

331 Approximation (1) is valid if the turbulent energy is mainly concentrated in
332 the region where the irrotational strain dominates vorticity. Exceptions on this
333 behaviour have been found and have motivated the development of alternative

334 models, like the Wall Adaptive Local Eddy-viscosity (WALE) model of Nicoud
 335 and Ducros [30] or the structure function model of Métais and Lesieur [25].
 336 Approximation (2) implies that the flow deformation rate can be represented
 337 by a linear function in each spatial point; thus it is a particularly regular
 338 function. This is equivalent to neglect the turbulent correction on advective
 339 velocity and continuity equation, hence the associated physical phenomena of
 340 turbophoresis and turbulent compressibility are not reproduced.

341 5 Numerical simulations

342 PSS and LES are compared on turbulence channel flow at $Re_\tau = 590$. The for-
 343 mer adopts a constant isotropic model for variance tensor, the latter adopts a
 344 constant Smagorinsky model for sub-grid scale viscosity. The Direct Numerical
 345 Simulation (DNS) of Moser *et al.* [28] is taken as reference.

346 5.1 Case geometry and settings

347 The channel is composed by two horizontal and parallel walls between which
 348 a shear flow develops. The dimensions in stream-wise (x), vertical (y) and
 349 span-wise (z) directions are $2\pi\delta \times \delta \times \pi\delta$, respectively. The flow is driven by
 350 a constant pressure gradient $\frac{\partial p}{\partial x} = -\rho u_\tau/\delta$. The Reynolds number based on
 351 the friction velocity u_τ is defined as $Re_\tau = u_\tau\delta/\nu$. The spatial variables are
 352 made non-dimensional as $y^+ = yu_\tau/\nu$, the velocity as $u^+ = u/u_\tau$, time as
 353 $t^+ = tu_\tau/\nu$. The characteristic flow time is estimated as $t_0 = U_0/2\pi\delta$, where
 354 U_0 is the bulk velocity in stream-wise direction.

355 The computational domain is discretised by $96 \times 96 \times 96$ points. They are
 356 uniformly distributed in stream-wise and span-wise directions, leading to a
 357 cell width $\Delta x^+ < 40$ and $\Delta z^+ < 20$, respectively. In vertical direction, the
 358 grid is stretched in a way such that the first cell is within $y^+ = 1$ and with 9
 359 cells in $y^+ \leq 11$; thus ensuring an accurate resolution of the boundary layer.
 360 The stretching is symmetric with respect to the channel centre plane $y = \delta$,
 361 and it is obtained with a double-side stretching function based on hyperbolic
 362 tangent:

$$363 \quad y(\xi) = \frac{1}{2} \left(1 + \frac{\tanh(\lambda(\xi - 1/2))}{\tanh(\lambda/2)} \right), \quad (20)$$

364 where ξ is the vertical coordinate of uniform point distribution and the stretch-
 365 ing factor is set to $\lambda = 5.25$.

366 Cyclic boundary conditions are set at the vertical boundaries, while velocity
 367 no-slip condition and pressure zero-gradient are imposed at the horizontal
 368 walls. All the cases are initialised with the instantaneous fields provided by a
 369 preliminary LES with constant Smagorinsky SGS model, that has reached the
 370 statistical steady state.

371 5.2 Algorithm and implementation

372 Simulations are performed taking advantage of the open-source software Open-
373 FOAM v. 2.3.0. This is a C++ library for computational fluid dynamics and
374 adopts the finite volume methods.

375 The LESs are carried out using the solver `pisoFoam` included in the stan-
376 dard software distribution. The implementation details on this basic solver can
377 be found in the official OpenFOAM documentation and in the work of Jasak
378 *et al.* [15]. The constant Smagorinsky SGS model is provided by OpenFOAM,
379 and its correct implementation was checked.

380 Two PSSs are performed using the code `pseudoStochasticPisoFoam` , a
381 home-made solver developed by the authors within the Fluminance research
382 group at INRIA Rennes (France). The non-conservative form of pseudo-stochastic
383 governing equations (5) are solved employing the Pressure-Implicit with Split-
384 ting of Operators (PISO) algorithm proposed by Issa *et al.* [14] and Oliveira
385 & Issa [32].

386 Variables are discretised in space with a second-order central difference
387 scheme, while time integration is performed using an implicit Euler backward
388 scheme. Such a scheme employs the variables at the previous two time steps,
389 leading to a second order accuracy. Globally, the numerical solvers are second-
390 order accurate in time and space. The time advancement fulfils the Courant-
391 Friedrichs-Lewy condition $Co < 0.5$. The Courant number is computed as
392 $Co = \Delta t |v| / \delta x$, where: Δt is the time step, $|v|$ is the velocity magnitude
393 through the cell, δx is the cell length. The model constants are chosen to be
394 $c_s^2 = c_m / 2 = 0.004225$, and for PSS $v = w^*$ while for LES $w^* = u$.

395 5.3 Results discussion

396 The simulations are run till the statistical steady state is reached, then they
397 are re-run for an additional period of $12t_0$ where the statistics are collected.
398 The quantities are averaged in time and in space along span-wise and stream-
399 wise directions, and exploiting the domain symmetry in vertical direction. The
400 angular brackets $\langle \psi \rangle$ denote the average in time and wall-parallel directions
401 for a generic variable ψ .

402 *First and second order statistics*

403 The first and second order statistics of the velocity field are analysed.

404 Figure 1 top-panel reports the mean non-dimensional stream-wise velocity
405 along the wall coordinate. PSS and LES lead to similar profiles in the near-wall
406 region ($y^+ < 30$), while the former exhibits slightly lower values in the log-law
407 region ($y^+ > 30$). They underestimate the velocity magnitude at the centre
408 channel and, as expected, both are not accurate in reproducing the boundary
409 layer profile. This is a well known shortcoming of Smagorinsky model when c_s^2
410 is constant, and it is inherited by the constant isotropic model.

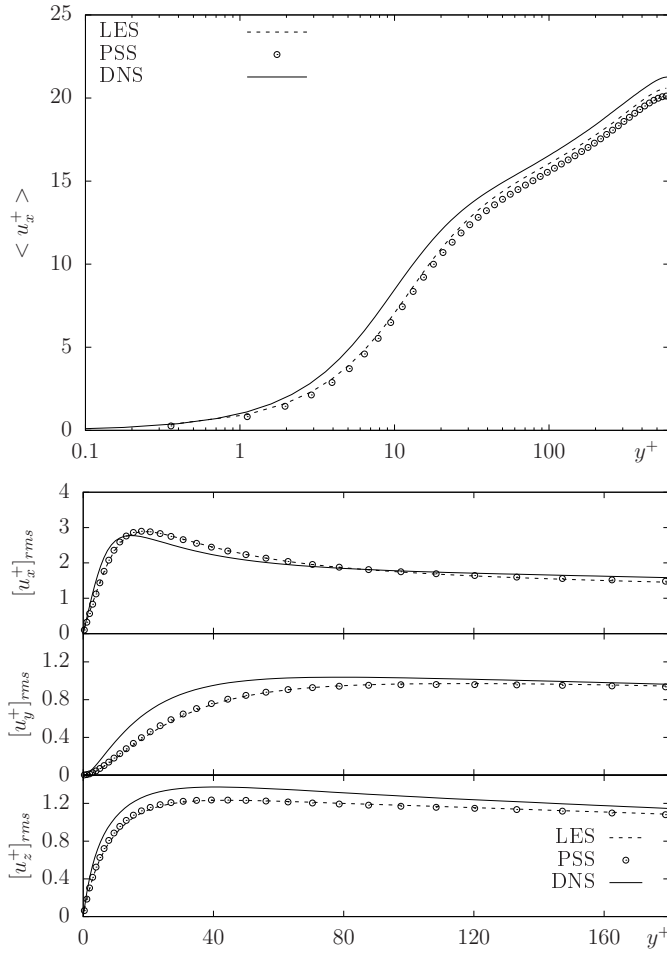


Fig. 1 First and second order statistics of velocity field versus non-dimensional vertical coordinate (wall coordinate). Top panel: non-dimensional mean stream-wise velocity. Bottom panel: non-dimension velocity root-mean square. Reference DNS by [28].

411 Figure 1 bottom-panel displays the velocity RMS components. If ψ is a
 412 generic variable, we denote $[\psi]_{rms} = \sqrt{\langle \psi'^2 \rangle}$ the root-mean square, where
 413 $\psi' = \psi - \langle \psi \rangle$ is the instantaneous fluctuation. Both PSS and LES collapse on
 414 the same profiles.

415 Because the isotropic model is very similar to the Smagorinsky model, an
 416 improvement of accuracy by the PSS is not expected. The interest of this
 417 validation is to prove that the pseudo-stochastic model is as accurate as the
 418 state-of-the-art LES methodologies, despite its derivation relies to a substan-
 419 tially different framework and its governing equations include several extra
 420 terms, which are analysed in the following sections.

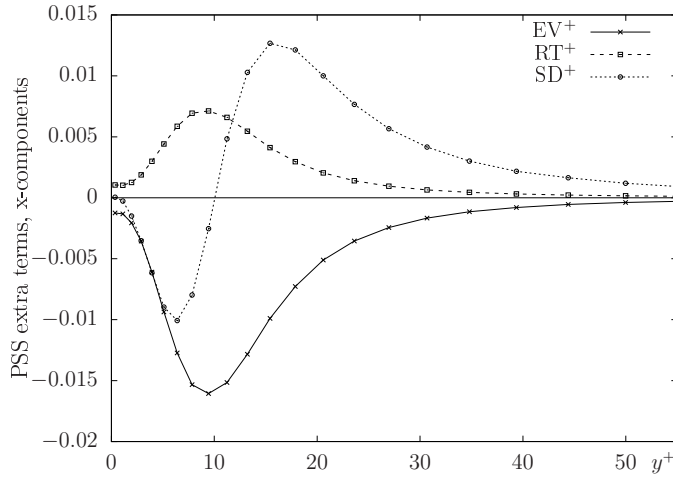


Fig. 2 Mean value of non-dimensional terms appearing in the pseudo-stochastic model with constant isotropic model, equation (19): component x along the wall-normal coordinate. EV, eddy-viscosity terms; RT, rotational term; SD, strain-rate diffusion.

421 *Effects of the extra terms in PSS*

422 The LES constant Smagorinsky model and the PSS constant isotropic model
 423 lead to similar governing equations, but the latter has some additional terms
 424 not present in the former: the eddy-viscosity terms (EV), the rotational term
 425 (RT) and the strain-rate diffusion (SD) defined in equation (19). The influence
 426 of such terms is checked.

427 Figure 2 shows the x -component of the above-mentioned terms (averaged)
 428 versus the wall coordinate. They are made non-dimensional by u_τ^3/ν . In LES,
 429 the term EV accounts for all sub-grid scale effects and represents a negative
 430 turbulent diffusion near the wall. In the PSS constant isotropic model, two
 431 other terms come into play: SD is negative in the region $y^+ < 10$, while it
 432 shows positive value at $y^+ > 10$; RT exhibits a positive contribution against
 433 the negative one of EV. The three terms become negligible in the log-law
 434 region; hence, the SUS model acts mainly at the near-wall region. The point
 435 $y^+ = 10$, located in the buffer layer, is of particular interest: approximately
 436 at this height, EV and RT reach the minimum and maximum (respectively),
 437 while SD changes sign. Globally, the RT and SD terms reduce the negative
 438 contribution of EV to the velocity equations in the buffer region, eventually
 439 producing a positive turbulent diffusion.

440 *Turbulent advection and compressibility*

441 Figure 3 presents the non-dimensional turbulent advection velocity $u_{TA}^+ =$
 442 u_{TA}/u_τ and the turbulent compressibility $\Phi_{TC}^+ = \Phi_{TC}u_\tau^2/\nu$ are scrutinised. The
 443 stream-wise component of u_{TA} is practically zero, as well as the span-wise com-
 444 ponent; thus they are not displayed. The vertical component profile reveals low

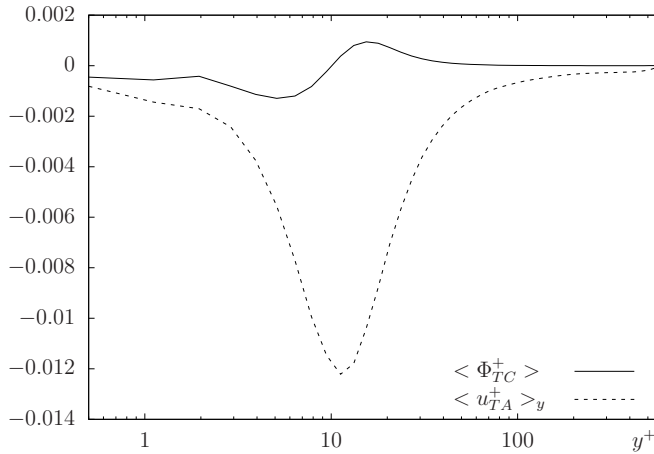


Fig. 3 Mean value of non-dimensional turbulent advection (12) and compressibility (13) appearing in the pseudo-stochastic model with constant isotropic model: x -component along the wall coordinate.

445 negative values, with a climax at $y^+ \cong 10$. Quantitatively, the turbulent ad-
 446 vection is not strong enough to produce remarkable results on the mean flow;
 447 however, it generates a weak vertical velocity w_y directed from the center to
 448 the wall of the channel (not reported). Hence, u_{TA} is qualified as a weak tur-
 449 bophoresis velocity: it advects the flow from the buffer region to the log-law
 450 region, i.e. in the direction of decreasing turbulence level (estimated by the
 451 velocity RMS intensity). The turbulent compressibility Φ_{TC} assumes negative
 452 values in the viscous sub-layer and positive values in the buffer layer. Else-
 453 where, it is practically zero. In light of equation (11), this behaviour is related
 454 to the presence of a turbulent fluid compression and expansion, respectively.
 455 Additional insight on this phenomenon is gained visualising the Φ_{TC} instanta-
 456 neous values.

457 Figure 4 displays the Φ_{TC} negative (blue) and positive (orange) isosurfaces
 458 near the bottom wall, at an instantaneous flow configuration. They are organ-
 459 ised in spots, confined in the near-wall region and elongated in the stream-
 460 wise direction. In accordance with the Φ_{TC} mean profile, the negative spots
 461 are closer to the wall ($y^+ < 10$), while the positive one are immediately above
 462 ($10 < y^+ < 20$). The shape and the location of the isosurfaces suggest a corre-
 463 lation with the *streaks* structures that characterises turbulent wall flows. The
 464 streaks are generated in a region of low velocity, very close to the wall, ap-
 465 proximately at $y^+ \simeq 5$. They are elongated in the stream-wise direction, with
 466 a characteristic length of $\Delta x^+ \cong 1000$ and a span-wise period of $\Delta z^+ \cong 100$.
 467 This estimation can vary with respect to the wall distance, see Smith & Metz-
 468 zler [44]. Despite their widespread presence, there is no clear consensus on
 469 the streak formation mechanism and multiple theories have been proposed in
 470 literature, see Chernyshenko & Baig [6]. The Φ_{TC} isosurfaces have, overall, the

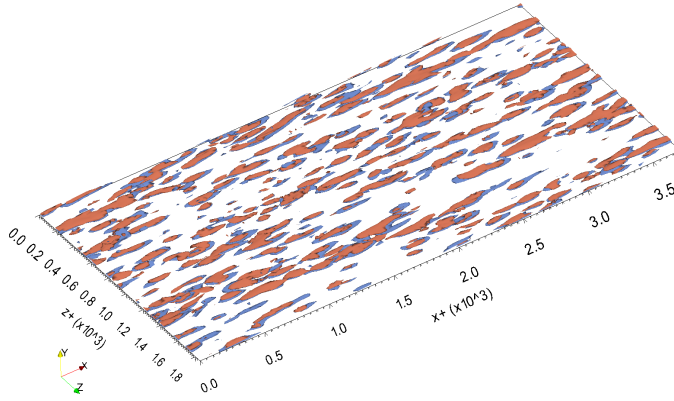


Fig. 4 Positive and negative isosurfaces of Φ_{TC} near the bottom wall at an instantaneous flow configuration. Orange: isosurface at $\Phi_{TC}^+ = 3.5/\text{times}10^{-4}$. Blue: isosurface at $\Phi_{TC}^+ = -3.5/\text{times}10^{-4}$.

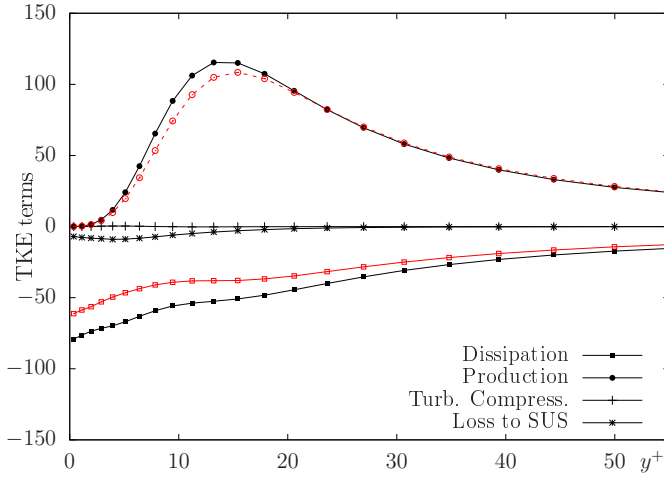


Fig. 5 Selected contributions to the pseudo-stochastic TKE budget versus wall-normal coordinate. The TKE terms are labelled as in equation (8). Results of three simulations are displayed: PSS with constant isotropic model, black lines with solid symbols; LES with constant Smagorinsky model, red lines with empty symbols.

471 same stream-wise extension and span-wise period. Also, the negative spots are
 472 located at the same height at which steaks are triggered. Therefore, these two
 473 structures appears to be related.

474 *Resolved turbulent kinetic budget*

475 The pseudo-stochastic TKE budget (8) is finally scrutinised for PSS and LES
 476 simulations

477 Figure 5 shows selected terms of the TKE budget. Production and dissipa-
478 tion profiles are similar for PSS and LES, but the former appears to be more
479 effective in energy dissipation in near-wall region and has a higher production
480 of TKE in the range $5 < y^+ < 20$. In the PSS, the turbulent compression
481 term is almost zero and does not contribute to the budget; while the loss due
482 to SUS presents slightly negative values mainly localised in the viscous layer.
483 Hence, it contributes to global energy dissipation.

484 6 Conclusions

485 The pseudo-stochastic simulation (PSS) methodology introduced by Mémin [24]
486 is analysed theoretically and numerically, through a direct comparison with
487 the classical large-eddy simulations (LES) approach. The PSS model is based
488 on an innovative decomposition of the fluid-particle trajectory in a drift dis-
489 placement and a stochastic perturbation. The former reproduces the mean
490 flow, the later accounts for the turbulent perturbations which are modeled
491 as a Brownian motion. Imposing such a decomposition, together with a reg-
492 ularity assumption on the drift velocity, a set of deterministic and stochastic
493 equations of motion are derived using stochastic calculus; then, the pseudo-
494 stochastic equations are obtained by neglecting the solution of stochastic equa-
495 tions and closing the system by physical assumptions. The result is a new set
496 of governing equations which includes extra terms deriving from the stochas-
497 tic modeling of turbulence. The PSS model is found to be a generalisation of
498 the classical Navier-Stokes equations, and reproduces phenomena usually not
499 considered: turbophoresis and turbulent compressibility.

500 The PSS of turbulent channel flow at $Re_\tau = 590$ is performed, together
501 with the LES with constant Smagorinsky sub-grid scale model. For a better
502 comparison, a closure model analogous to the Smagorinsky one is used for the
503 PSS. However, it is shown that this last does not rely on the eddy-viscosity hy-
504 potheses, hence it is not affected by its shortcomings. The PSS does not show
505 improvement in first and second order statistics, possibly because of the sim-
506 ple expression of a_{ij} , but reproduces additional features: a weak turbophoresis
507 is detected in the buffer region, while a turbulent compression and expansion
508 is identified in the viscous and buffer layer (respectively). This quantity ap-
509 pears to be related to the streaks, turbulent structures appearing near the wall
510 region.

511 Finally, the pseudo-stochastic model is a generalisation of the LES eddy-
512 viscosity model and describes a richer physics. Overall, it represents a promis-
513 ing approach for simulation of turbulent flows: the mathematical analysis here
514 reported gives a clear physical interpretation of the model, supported by nu-
515 merical results.

516 A . Formal derivation of stochastic model

517 The mathematical conditions under which this derivation is consistent are reported in [9, 26,
518 27]. An introduction to the mathematical framework in which the present model is developed
519 can be found in  ksendal [31] and Kunita [18].

520 A.1 Trajectory and stochastic velocity definitions

521 As already mentioned, expression (1) has to be understood in an integral sense:

$$522 \quad X_t^i = X_0^i + \int_0^t w_i(X_s, s) ds + \int_0^t d\eta_s^i(X_s), \quad (21)$$

523 where the It  stochastic integral is used to integrate the random process. The process $X_t^i(x_0)$
524 is a semimartingale defined for each spatial point $x_0 \in \Omega$ and time $t \in T \subseteq \mathbb{R}^+$ in an
525 appropriate probability space.

526 The stochastic velocity in equation (3) is a symbolic expression that is defined as a weak
527 derivative of the random displacement:

$$528 \quad \int h(t) \dot{\eta}_t^i(x) dt = \int h'(t) \eta_t^i(x) dt, \quad (22)$$

529 for each h test function; see also [31].

530 A.2 The stochastic Reynolds transport theorem

531 Being the velocity field a stochastic process, the governing equations of fluid dynamics
532 cannot be recovered using deterministic calculus, ref. [24, 27]. In this concern, the key point
533 is to give an expression of the *Reynolds transport theorem* (RTT) for stochastic quantities.
534 Subsequently, the stochastic Navier-Stokes equations are found imposing conservation of
535 mass and momentum.

536 **Theorem 1 (Stochastic RTT)** *Let us consider a physical quantity $q(x, t)$ within a ma-*
537 *terial volume $V(t) \subset \mathbb{R}^3$, transported by a stochastic flow of the form (1) and such that it*
538 *can be written as a semimartingale of the type:*

$$539 \quad q(x, t) = q(x, 0) + \int_0^t g(x, s) ds + \int_0^t \int_{\Omega} f_k(x, y, s) dB_s^k(y) dy ds, \quad (23)$$

540 where g, f are processes of bounded-variation and the It  integral are employed. If the fol-
541 lowing properties holds:

- 542 1. symmetric diffusion tensor: $\sigma_{ij} = \sigma_{ji}$,
- 543 2. solenoidal diffusion tensor: $\frac{\partial}{\partial x_i} \sigma_{ij}(x, y, t) = 0$ for all j ,
- 544 3. conserved quantity: $dq(X_t, t) = 0$,

then the stochastic RTT has an explicit differential form that reads:

$$d \int_{V(t)} q(x, t) dx = \int_{V(t)} \left[\partial_t q + \frac{\partial(qw_i)}{\partial x_i} dt - \frac{1}{2} \frac{\partial^2(qa_{ij})}{\partial x_i \partial x_j} dt + \frac{\partial q}{\partial x_i} d\eta_t^i \right] dx, \quad (24)$$

545 where ∂_t is the differential with respect to the second variable, and d denotes the total time
546 increment at a fixed spatial point.

547 Assumption (1) greatly simplifies the computation and can be justified *a posteriori*: it implies
 548 that the variance tensor a_{ij} is symmetric, a desirable properties in light of its physical
 549 interpretation (see section 3.1). Therefore, this assumption is considered reasonable in the
 550 fluid dynamics context; however it is not mandatory, see [37]. Hypothesis (2) can be removed,
 551 but the stochastic RTT expression assumes a more complex formulation. It is found that this
 552 constrain is naturally satisfied by fluids where density is constant in space (see section A.3),
 553 thus formula (24) is directly applied when the flow is incompressible or when the Boussinesq
 554 approximation is applied. On the contrary, an explicit formula has not been derived for a
 555 generic non-conserved quantity; hence hypothesis (3) is essential.

556 Notice that equation (24) reduces to the classical RTT when the stochastic contribu-
 557 tion in equation (1) is suppressed. This happens e.g. when $\sigma_{ij} = 0$ and, consequently, the
 558 martingale η_t^i as well as the variance tensor are identically zero.

559 A concise derivation of the stochastic RTT is now presented. A generic random process
 560 $\phi(x, t)$ is expressed hereafter as a semimartingale of the form:

$$562 \quad \phi(x, t) = \phi(x, 0) + \int_0^t g(x, s) ds + \int_0^t \int_{\Omega} f_k(x, y, s) dB_s^k(y) dy ds, \quad (25)$$

563 where g, f are processes of bounded-variation and the Itô integral are used.

Proposition 1 (Differential of transported process) *Let us consider ϕ a semimartin-
 gale of the type (25), sufficiently regular in space (bounded spatial gradient, two times deriv-
 able). If it is transported by a flow of the form (21); then, the time total-differential of ϕ is
 expressed by:*

$$d\phi(X_t, t) = \partial_t \phi + \frac{\partial \phi}{\partial x_i} dX_t^i + \frac{1}{2} a_{ij}(X_t, t) \frac{\partial^2 \phi}{\partial x_i \partial x_j} dt + \int_{\Omega} \sigma_{ij}(X_t, y, t) \frac{\partial}{\partial x_i} f_j(X_t, y, t) dy dt, \quad (26)$$

564 where ∂_t is the time partial-differential (i.e. with respect to second variable), and a_{ij} is the
 565 variance tensor defined by equation (4).

Proof: The Itô-Wentzell formula is used to differentiate (in time) the transported process
 $\phi(X_t, t)$, corresponding to a composition of two processes. It reads:

$$d\phi(X_t, t) = \partial_t \phi + \frac{\partial \phi}{\partial x_i} dX_t^i + \frac{1}{2} d\langle X^i, X^j \rangle_t \frac{\partial^2 \phi}{\partial x_i \partial x_j} + d\left\langle \frac{\partial \phi}{\partial x_i}, X^i \right\rangle_t, \quad (27)$$

566 where the angular brackets denote the quadratic variation operation; e.g. see Le Gall [19] for
 567 an extended presentation. The following properties of the quadratic variation are recalled:

- 568 1. is symmetric and bilinear;
- 569 2. if g is a process of bounded-variation: $\langle g, B^k \rangle_t = 0$
- 570 3. if f is deterministic function: $\langle f B^i, B^j \rangle_t = f \langle B^i, B^j \rangle_t$
- 571 4. singularity: $d\langle B^i(y), B^j(z) \rangle_t = \delta(y - z) \delta_{ij} dt$

where B_t is a cylindrical Wiener process, $\delta(x)$ is the Dirac function and δ_{ij} is the Kronecker
 symbol. Using these properties, the third and fourth terms in equation (27) are written
 explicitly. The third term is directly computed:

$$d\langle X^i, X^j \rangle_t = \int_{\Omega} \sigma_{ik}(X_t, y, t) \sigma_{jk}(X_t, y, t) dy dt = a_{ij}(X_t, t) dt. \quad (28)$$

In the fourth term, the gradient of ϕ is obtained differentiating equation (25):

$$\frac{\partial}{\partial x_i} \phi(X_t, t) = \frac{\partial \phi_0}{\partial x_i} + \int_0^t \frac{\partial}{\partial x_i} g(X_s, s) ds + \int_0^t \int_{\Omega} \frac{\partial}{\partial x_i} f_k(X_s, y, s) dB_s^k(y) dy ds, \quad (29)$$

then, the last term in (27) is rewritten as:

$$d\left\langle \frac{\partial \phi}{\partial x_i}, X^i \right\rangle_t = \int_{\Omega} \sigma_{ij}(X_t, y, t) \frac{\partial}{\partial x_i} f_j(X_t, y, t) dy dt. \quad (30)$$

572 Substituting formula (28) and (29) in equation (27), expression (26) is recovered. \square

Proposition 2 (Differential of transported and conserved process) *Let us consider a stochastic process ϕ of the type (25). If such a process is transported by a stochastic flow (21) and is conserved, i.e. $d\phi(X_t, t) = 0$, then:*

$$\partial_t \phi(X_t, t) = -\frac{\partial \phi}{\partial x_i} w_i dt + \frac{1}{2} a_{ij} \frac{\partial^2 \phi}{\partial x_i \partial x_j} dt + \int_{\Omega} \frac{\partial \phi}{\partial x_k} \frac{\partial \sigma_{kj}}{\partial x_i} \sigma_{ij} dy dt - \int_{\Omega} \frac{\partial \phi}{\partial x_i} \sigma_{ik} dB_t^k dy. \quad (31)$$

573 *This formula expresses the time variation along a fluid-particle trajectory.*

Proof: If $\phi(X_t, t)$ is conserved, then equation (26) can be re-arranged as follows:

$$\begin{aligned} \partial_t \phi(X_t, t) = & -\frac{\partial \phi}{\partial x_i} w_i dt - \int_{\Omega} \frac{\partial \phi}{\partial x_i} \sigma_{ik}(X_t, y, t) dB_t^k(y) dy - \\ & - \frac{1}{2} a_{ij} \frac{\partial^2 \phi}{\partial x_i \partial x_j} dt - \int_{\Omega} \sigma_{ij}(X_t, y, t) \frac{\partial}{\partial x_i} f_j(X_t, y, t) dy dt. \end{aligned} \quad (32)$$

An expression of $\partial_t \phi$ is obtained also from (25), and is compared with formula (32). Exploiting the unique decomposition of the semimartingales, one obtains:

$$g(X_t, t) = -\frac{\partial \phi}{\partial x_i} w_i - \frac{1}{2} a_{ij} \frac{\partial^2 \phi}{\partial x_i \partial x_j} - \int_{\Omega} \sigma_{ij}(X_t, y, t) \frac{\partial}{\partial x_i} f_j(X_t, y, t) dy, \quad (33)$$

574 and the following implicit formula for f :

$$575 \quad \int_{\Omega} \left[f_k(X_t, y, t) + \frac{\partial \phi(X_t, t)}{\partial x_i} \sigma_{ik}(X_t, y, t) \right] dB_t^k(y) dy = 0. \quad (34)$$

576 This latter holds for every Brownian motion dB_t^k , thus:

$$577 \quad f_k(X_t, y, t) = -\frac{\partial \phi(X_t, t)}{\partial x_i} \sigma_{ik}(X_t, y, t). \quad (35)$$

578 Substituting formula (35) in equation (32) the final expression (31) is obtained. \square

579

580 Notice that a general form of a conserved semimartingale can be found by substituting equation (33) and (35) in formula (25).

581 Translating equation (31) from Lagrangian to Eulerian coordinates and rearranging the
582 second and third terms in the left-hand side, one obtains the expression of the material
583 derivative (in differential form) within the stochastic framework.
584

Proposition 3 (Stochastic transport operator) *If ϕ is a stochastic process of the type (25), transported by a stochastic flow (21) and conserved, then the stochastic material derivative in differential form is:*

$$\begin{aligned} D\phi(x, t) = & \partial_t \phi + (w_i dt + d\eta_t^i) \frac{\partial \phi}{\partial x_i} - \frac{1}{2} \frac{\partial}{\partial x_i} \left(a_{ij} \frac{\partial \phi}{\partial x_j} \right) dt \\ & - \left(\frac{1}{2} \frac{\partial a_{ij}}{\partial x_i} - \int_{\Omega} \sigma_{kj} \frac{\partial \sigma_{ij}}{\partial x_i} dy \right) \frac{\partial \phi}{\partial x_j} dt, \end{aligned} \quad (36)$$

585 *which is reported in [37] as the stochastic transport operator for a conserved quantity.*

586 The derivation of Stochastic RTT is now summarised. Let us consider a generic physical
587 quantity, mathematically expressed by a stochastic scalar process $q(x, t)$ that satisfies the
588 hypotheses of Stochastic RTT. The solution of transport equation is found in the space of
589 weak solutions.
590

Proof (Stochastic RTT): Consider a control volume $V(t)$ and a test function $\varphi(x, t)$ in the space domain Ω such that: it has compact support on $V(t)$, it is conserved and satisfies (25). Then, the weak transport equation for q reads:

$$d \int_{V(t)} q(x, t) \varphi(x, t) dx = \int_{\Omega} [\varphi \partial_t q + q \partial_t \varphi + d \langle q, \varphi \rangle_t] dx, \quad (37)$$

applying the Itô integration by part and passing to the integral on Ω because φ has compact support on V . The last term on the right-hand side needs to be explicit. An expression of q and φ is given by the semimartingale decomposition (25):

$$\varphi = \varphi(x, 0) + \int_0^t g(x, s) ds + \int_0^t \int_{\Omega} f_j(x, y, s) dB_s^j dy, \quad (38)$$

$$q = q(x, 0) + \int_0^t h(x, s) ds + \int_0^t \int_{\Omega} \kappa_j(x, y, s) dB_s^j dy, \quad (39)$$

where explicit formulae for g, h, f, κ are given, see proof of Proposition 2. Using these expressions to compute the quadratic variation, we get:

$$d \langle q, \varphi \rangle_t = d \int_{\Omega} \left\langle \int_{\Omega} \kappa_i dB^i dy, \int_{\Omega} f_j dB^j dz \right\rangle_t = \frac{\partial q}{\partial x_k} \frac{\partial \varphi}{\partial x_\ell} a_{k\ell} dt, \quad (40)$$

The same expressions are differentiated to express $\partial_t q(x, t)$ and $\partial_t \varphi(x, t)$, that are substituted in the transport equation (37) together with formula (40). Subsequently, φ is used to compute the weak derivative and gathered; the final equation reads:

$$d \int_{\Omega} q(x, t) \varphi(x, t) dx = \int_{\Omega} \varphi \left[\partial_t q + \frac{\partial q w_i}{\partial x_i} dt + \frac{1}{2} \frac{\partial^2}{\partial x_i \partial x_j} (q a_{ij}) dt - \frac{\partial}{\partial x_k} \int_{\Omega} q \frac{\partial \sigma_{kj}}{\partial x_i} \sigma_{ij} dy dt + \frac{\partial}{\partial x_i} (q d\eta_t^i) - \frac{\partial}{\partial x_\ell} \left(\frac{\partial q}{\partial x_k} a_{k\ell} \right) dt \right] dx. \quad (41)$$

Equation (41) is valid for every test function φ with compact support in $V(t)$, thus:

$$d \int_V q(x, t) dx = \int_V \left[\partial_t q + \frac{\partial q w_i}{\partial x_i} dt + \frac{\partial}{\partial x_i} (q d\eta_t^i) + \frac{1}{2} q \left\| \frac{\partial \sigma}{\partial x} \right\|^2 dt - \frac{1}{2} \int_{\Omega} \left(q \frac{\partial \sigma_{ik}}{\partial x_j} \frac{\partial \sigma_{kj}}{\partial x_i} + \frac{\partial^2 q}{\partial x_i \partial x_j} \sigma_{ik} \sigma_{kj} + 2 \sigma_{ij} \frac{\partial q}{\partial x_k} \frac{\partial \sigma_{kj}}{\partial x_i} \right) dy dt \right] dx, \quad (42)$$

591 where the terms are rearranged and the definition of variance tensor is used to simplify
592 some terms. Equation (42) is the general form of Stochastic RTT, that is quite complex and
593 eventually difficult to handle. One can notice that under the additional hypothesis that the
594 random term is solenoidal in space, i.e.

$$595 \quad \frac{\partial}{\partial x_i} d\eta_t^i(x) = 0 \quad \Leftrightarrow \quad \frac{\partial}{\partial x_i} \sigma_{ik}(x, y, t) \equiv 0, \quad (43)$$

where the if and only if statement holds because the Brownian motion is arbitrarily chosen, the equation (42) simplifies to:

$$d \int_V q(x, t) dx = \int_V \left[\partial_t q + \frac{\partial (q w_i)}{\partial x_i} dt - \frac{1}{2} \frac{\partial^2 (q a_{ij})}{\partial x_i \partial x_j} dt + \frac{\partial (q d\eta_t^i)}{\partial x_i} \right] dx, \quad (44)$$

596 that is the final form of Stochastic RTT. \square

597

598 In the following section, it is shown that the assumption of a solenoidal random turbu-
599 lence field is satisfied by incompressible fluids, thus the simpler equation (44) can be used
600 to derived the equation of motion.

601 It is worth noticing that the Stochastic RTT can be applied to all functions of the
602 form (25); specifically, to all process of bounded-variations that are a particular case of
603 semimartingale where the martingale term is zero.

604 A.3 Derivation of Stochastic Navier-Stokes equations

605 The derivation of governing equations for fluid flows is performed with a similar strategy as
606 in the classical framework, e.g. see [17].

607 *Conservation of mass*

If $\rho(x, t)$ is the mass density, then the conservation of mass is:

$$d \int_{V(t)} \rho dx = \int_{V(t)} \left[\partial_t \rho + \frac{\partial \rho w_i}{\partial x_i} dt + \frac{\partial}{\partial x_i} (\rho d\eta_t^i) + \frac{1}{2} \rho \left\| \frac{\partial \sigma}{\partial x} \right\|^2 dt \right] dx = 0, \quad (45)$$

$$- \frac{1}{2} \int_{\Omega} \left(\rho \frac{\partial \sigma_{ik}}{\partial x_j} \frac{\partial \sigma_{kj}}{\partial x_i} + \frac{\partial^2 \rho}{\partial x_i \partial x_j} \sigma_{ik} \sigma_{kj} + 2 \sigma_{ij} \frac{\partial \rho}{\partial x_k} \frac{\partial \sigma_{kj}}{\partial x_i} \right) dy dt \Big] dx = 0, \quad (46)$$

608 where the general form of Stochastic RTT (42) is used here. For an incompressible fluid,
609 density is constant $\rho(x, t) = \rho$ and the mass conservation equation simplifies accordingly.
610 The integral is then removed exploiting the arbitrariness of control volume:

$$611 \quad \frac{\partial w_i}{\partial x_i} dt + \frac{\partial}{\partial x_i} d\eta_t^i + \frac{1}{2} \left\| \frac{\partial \sigma}{\partial x} \right\|^2 dt - \frac{1}{2} \int_{\Omega} \frac{\partial \sigma_{ik}}{\partial x_j} \frac{\partial \sigma_{kj}}{\partial x_i} dy dt = 0. \quad (47)$$

Separating the processes of bounded-variation and the martingales, the following system is recovered:

$$\left(\frac{\partial w_i}{\partial x_i} + \frac{1}{2} \left\| \frac{\partial \sigma}{\partial x} \right\|^2 - \frac{1}{2} \int_{\Omega} \frac{\partial \sigma_{ik}}{\partial x_j} \frac{\partial \sigma_{kj}}{\partial x_i} dy \right) dt = 0, \quad \frac{\partial}{\partial x_i} d\eta_t^i = 0. \quad (48)$$

612 Equation (48) shows that for an incompressible fluid the Brownian term is solenoidal; thus,
613 the use of the simplified expression Stochastic RTT (44) is *a posteriori* justified for incom-
614 pressible fluids. Using the solenoidal constraint, equations (48) leads to the system:

$$615 \quad \frac{\partial}{\partial x_i} \left(w_i - \frac{1}{2} \frac{\partial}{\partial x_j} a_{ij} \right) = 0, \quad \frac{\partial}{\partial x_i} \sigma_{ik} = 0, \quad (49)$$

616 which expresses the conservation of mass.

617 *Conservation of momentum*

618 Two derivations are proposed, they are named Lagrangian and Eulerian for convenience of
619 notation. The former is based on the work of [27], the latter on that one of [24].

620

621 • LAGRANGIAN: The second Newton's law is:

$$622 \quad \frac{d}{dt} \rho U_i(X_t, t) = F_i(X_t, t), \quad (50)$$

623 where F_i are the forces acting on a fluid-particle. If I_i is the time integral of the forces (the
624 *impulse*), equation (50) is re-written in a differential form as $d\rho U_i = dI_i$. It is expressed in
625 a weak form as:

$$626 \quad \rho \int h dU_i(X_t, t) = \int h dI_i(X_t, t), \quad (51)$$

627 where h are test functions and ρ is constant. The left-hand side is:

$$628 \quad \rho \int h dU_i(X_t, t) = \rho \int h dw_i(X_t, t) - \rho \int h' d\eta_t^i, \quad (52)$$

629 then, the right-hand side of equation (51) must have the same structure, see [27]. Hence,
630 the impulse divides into two contributions and equation (51) becomes:

$$631 \quad \rho \int h dw_i(X_t, t) - \rho \int h' d\eta_t^i = \int h d\mathcal{J}_i - \int h' d\lambda_t^i. \quad (53)$$

Matching similar terms, we arrived at the following relations:

$$\rho dw_i = d\mathcal{J}_i, \quad d\eta_t^i = d\lambda_t^i. \quad (54)$$

632 Equations (54)-first is exploited to obtain the governing equation of motion, while (54)-
633 second states that the forces balance the contribution of random velocities. In Eulerial
634 framework, this latter reads:

$$635 \quad \rho Dw_i(x, t) = d\mathcal{J}_i(x, t), \quad (55)$$

636 Applying the stochastic transport operator (36) with the solenoidal constrain (49), one gets:

$$637 \quad Dw_i = \partial_t w_i + (w_j - \frac{1}{2} \frac{\partial a_{kj}}{\partial x_k}) \frac{\partial w_i}{\partial x_j} dt - \frac{1}{2} \frac{\partial}{\partial x_k} \left(a_{jk} \frac{\partial w_i}{\partial x_j} \right) dt + d\eta_t^j \frac{\partial w_i}{\partial x_j}, \quad (56)$$

while the impulse is determined by a physical analysis of the forces acting on the system,
as in the classical derivation:

$$d\mathcal{J}_i = -\frac{\partial}{\partial x_i} (pdt - d\xi_t) + \mu \frac{\partial^2}{\partial x_j \partial x_j} (dX_t^i) + \frac{\mu}{3} \frac{\partial}{\partial x_i} \frac{\partial}{\partial x_\ell} (dX_t^\ell) \quad (57)$$

$$= \left[-\frac{\partial p}{\partial x_i} + \mu \frac{\partial^2 w_i}{\partial x_j \partial x_j} + \frac{\mu}{3} \frac{\partial^2 w_\ell}{\partial x_i \partial x_\ell} \right] dt - \frac{\partial (d\xi_t)}{\partial x_i} + \mu \frac{\partial^2 (d\eta_t^i)}{\partial x_j \partial x_j} + \frac{\mu}{3} \frac{\partial^2 (d\eta_t^\ell)}{\partial x_i \partial x_\ell}, \quad (58)$$

639 with μ is the fluid viscosity, and pressure is written in a semimartingale form (25) where
640 $d\xi_t(x) = \int_\Omega \vartheta_i(x, y, t) dB_t^i(y) dy$ denotes the martingale contribution to pressure. Imposing
641 the equality (55) and using the unique decomposition of semimartingale, the governing equa-
642 tions (63) are recovered.

643
644 • EULERIAN: Once again, the momentum conservation is formulated in differential form. If
645 $\mathcal{J}_i(x, t)$ is the impulse of total forces per volume, the second law of mechanics reads:

$$646 \quad d \int_{V(t)} \rho U_i(x, t) dx = \int_{V(t)} d\mathcal{J}_i(x, t) dx. \quad (59)$$

The Stochastic RTT is applied to the left-hand side in order to get:

$$d \int_{V(t)} \rho U_i dx = \int_{V(t)} \rho \left[\partial_t w_i + \frac{\partial}{\partial x_j} (w_i w_j) dt - \frac{1}{2} \frac{\partial^2}{\partial x_s \partial x_k} (w_i a_{sk}) dt + \right. \\ \left. + \frac{\partial}{\partial x_j} (w_i d\eta_t^j) \right] dx + d \int_{V(t)} \rho \eta_t^i dx, \quad (60)$$

where the velocity decomposition (3) is employed. The impulse acting on $V(t)$ is expressed
by (58). Then, imposing equality (59) and separating the processes of bounded-variation to
the martingales, one obtains:

$$\partial_t w_i + \frac{\partial w_i w_j}{\partial x_j} dt - \frac{1}{2} \frac{\partial^2 (w_i a_{sk})}{\partial x_s \partial x_k} dt = -\frac{\partial p}{\partial x_i} dt + \nu \frac{\partial^2 w_i}{\partial x_j \partial x_j} dt + \frac{\nu}{3} \frac{\partial}{\partial x_i} \frac{\partial w_\ell}{\partial x_\ell} dt \quad (61)$$

with $\nu = \mu/\rho$ is the dynamic viscosity, and

$$d \int_{V(t)} \eta_t^i dx = \int_{V(t)} \left[-\frac{\partial}{\partial x_i} d\xi_t + \nu \frac{\partial^2}{\partial x_j \partial x_j} d\eta_t^i - d\eta_t^j \frac{\partial w_i}{\partial x_j} \right] dx \quad (62)$$

647 where the conservation of mass constrain (49) is applied to simplify the formula. Notice that
 648 the expected value of noise is zero because the random displacement is uncorrelated in time.
 649 Then, the integral at the right-hand side can be interpreted as a spatial empirical mean of
 650 zero-mean random process, and have to be null. With this simplification, the system (63) of
 651 fluid dynamics equations is obtained.

652 Finally, the stochastic model for an incompressible (Newtonian) fluid reads:

$$\begin{cases}
 \frac{\partial w_i}{\partial t} + \frac{\partial(w_j w_i)}{\partial x_j} = -\frac{\partial p}{\partial x_i} + \nu \frac{\partial^2 w_i}{\partial x_j \partial x_j} + \frac{\nu}{3} \frac{\partial}{\partial x_i} \frac{\partial w_\ell}{\partial x_\ell} + \frac{1}{2} \frac{\partial^2 (a_{sk} w_i)}{\partial x_s \partial x_k} \\
 \frac{\partial}{\partial x_i} \left(w_i - \frac{1}{2} \frac{\partial}{\partial x_j} a_{ij} \right) = 0 \\
 \frac{1}{\rho} \frac{\partial}{\partial x_i} d\xi_t = \nu \frac{\partial^2}{\partial x_j \partial x_j} d\eta_t^i - d\eta_t^j \frac{\partial w_i}{\partial x_j} \\
 \frac{\partial}{\partial x_i} d\eta_t^i = 0
 \end{cases} \quad (63)$$

655 The system is composed by two coupled sets of deterministic and stochastic non-linear
 656 partial differential equations, in the unknowns w_i and σ_{ij} . The pseudo-stochastic model is
 657 obtained by avoiding the resolution of the last two stochastic equations, and closing the
 658 system by providing an expression a_{ij} through physical assumptions.

659 Let us also outline that the system (63) has been obtained under the assumption that
 660 the drift velocity is of bounded variation. Removing this assumption, the separation of
 661 the regular and the stochastic terms cannot be performed anymore. Hence, one obtains
 662 a fully stochastic Navier-Stokes composed by stochastic partial differential equations. For
 663 geophysical flows (for isochoric flows in general), the continuity equations is also stochastic;
 664 see [37].

665 References

- 666 1. Bauer, W., Haag, O., Hennecke, D.: Accuracy and robustness of nonlinear eddy viscosity
 667 models. *International Journal of Heat and Fluid Flow* **21**(3), 312–319 (2000). DOI
 668 doi.org/10.1016/S0142-727X(00)00015-1
- 669 2. Brzeźniak, Z., Capiński, M., Flandoli, F.: Stochastic partial differential equations and
 670 turbulence. *Mathematical Models and Methods in Applied Sciences* **1**(01), 41–59 (1991)
- 671 3. Chandramouli, P., Heitz, D., Laizet, S., Mémin, E.: Coarse large-eddy simulations in
 672 a transitional wake flow with flow models under location uncertainty. *Computers and*
 673 *Fluids* **168**, 170 – 189 (2018). DOI doi.org/10.1016/j.compfluid.2018.04.001
- 674 4. Chapron, B., Drian, P., Mémin, E., Resseguier, V.: Largescale flows under location
 675 uncertainty: a consistent stochastic framework. *Quarterly Journal of the Royal Meteorological Society* **144**(710), 251–260 (2017). DOI 10.1002/qj.3198
- 676 5. Chasnov, J.R.: Simulation of the kolmogorov inertial subrange using an improved
 677 subgrid model. *Physics of Fluids A: Fluid Dynamics* **3**(1), 188–200 (1991). DOI
 678 10.1063/1.857878
- 679 6. Chernyshenko, S.I., Baig, M.F.: The mechanism of streak formation in near-wall turbu-
 680 lence. *Journal of Fluid Mechanics* **544**, 99–131 (2005). DOI 10.1017/S0022112005006506
- 681 7. Deardorff, J.W.: A numerical study of three-dimensional turbulent channel flow at large
 682 reynolds numbers. *Journal of Fluid Mechanics* **41**(2), 453480 (1970). DOI 10.1017/
 683 S0022112070000691
- 684 8. Durbin, P.A., Speziale, C.G.: Realizability of second-moment closure via stochastic anal-
 685 ysis. *Journal of Fluid Mechanics* **280**, 395–407 (1994). DOI 10.1017/S0022112094002983
- 686 9. Flandoli, F.: An Introduction to 3D Stochastic Fluid Dynamics, pp. 51–150. Springer
 687 Berlin Heidelberg, Berlin, Heidelberg (2008). DOI 10.1007/978-3-540-78493-7_2
- 688 10. Flandoli, F.: The interaction between noise and transport mechanisms in pdes. *Milan*
 689 *Journal of Mathematics* **79**(2), 543–560 (2011). DOI 10.1007/s00032-011-0164-5

- 691 11. Frederiksen, J.S., O’Kane, T.J., Zidikheri, M.J.: Subgrid modelling for geophysical
692 flows. *Philosophical Transaction of Royal Society A* **371**(1982) (2013)
- 693 12. Harouna, S.K., Mémin, E.: Stochastic representation of the reynolds transport theorem:
694 Revisiting large-scale modeling. *Computers and Fluids* **156**, 456 – 469 (2017)
- 695 13. Holm, D.D.: Variational principles for stochastic fluid dynamics. *Proceedings of the*
696 *Royal Society of London A: Mathematical, Physical and Engineering Sciences* **471**(2176)
697 (2015). DOI 10.1098/rspa.2014.0963
- 698 14. Issa, R.I., Gosman, A.D., Watkins, A.P.: The computation of compressible and in-
699 compressible recirculating flows by a non-iterative implicit scheme. *J. Computational*
700 *Physics* **62**, 66 (1986)
- 701 15. Jasak, H., Weller, H., Gosman, A.: High resolution NVD differencing scheme for arbi-
702 trarily unstructured meshes. *Int. J. Numer. Meth. Fluids* **31**, 431–449 (1999)
- 703 16. Kraichnan, R.H.: Dynamics of nonlinear stochastic systems. *Journal of Mathematical*
704 *Physics* **2**(1), 124–148 (1961). DOI 10.1063/1.1724206
- 705 17. Kundu, P., Cohen, I.M.: *Fluid Mechanics*, third edn. Elsevier Academic Press (2004)
- 706 18. Kunita, H.: *Stochastic Flows and Stochastic Differential Equations*. Cambridge Univer-
707 sity Press (1997)
- 708 19. Le Gall, J.F.: *Brownian Motion, Martingales, and Stochastic Calculus*. Springer Inter-
709 national Publishing (2016). DOI doi.org/10.1007/978-3-319-31089-3
- 710 20. Leith, C.E.: Stochastic backscatter in a subgridscale model: Plane shear mixing layer.
711 *Physics of Fluids A: Fluid Dynamics* **2**(3), 297–299 (1990). DOI 10.1063/1.857779
- 712 21. Lesieur, M.: *Turbulence in Fluids, Fluid Mechanics and Its Applications*, vol. 84.
713 Springer Netherlands (2008). DOI 10.1007/978-1-4020-6435-7
- 714 22. Leslie, D.C.: *Developments in the theory of turbulence*. Oxford, Clarendon Press (1973)
- 715 23. Lilly, D.K.: The representation of small-scale tubulence in numerical simulation exper-
716 iments. In: H. H. Goldstine, *Proceedings of IBM Scientific Computing Symposium on*
717 *Environmental Sciences* pp. 195–210 (1967)
- 718 24. Mémin, E.: Fluid flow dynamics under location uncertainty. *Geophysical and Astro-*
719 *physical Fluid Dynamics* **108**(2), 119–146 (2014). DOI 10.1080/03091929.2013.836190
- 720 25. Métais, O., Lesieur, M.: Spectral large-eddy simulation of isotropic and stably strat-
721 ified turbulence. *Journal of Fluid Mechanics* **239**, 157–194 (1992). DOI 10.1017/
722 S0022112092004361
- 723 26. Mikulevicius, R., Rozovskii, B.L.: *On Equations of Stochastic Fluid Mechanics*.
724 *Trends in Mathematics*. Birkhäuser, Boston, MA (2001). DOI doi.org/10.1007/
725 978-1-4612-0167-0_15. In: Hida T., Karandikar R.L., Kunita H., Rajput B.S., Watanabe
726 S., Xiong J. (eds) *Stochastics in Finite and Infinite Dimensions*.
- 727 27. Mikulevicius, R., Rozovskii, B.L.: Stochastic navier-stokes equations for turbulent
728 flows. *SIAM J. Mathematical Analysis* **35**(5), 1250–1310 (2004). DOI doi.org/10.1137/
729 S0036141002409167
- 730 28. Moser, R.D., Kim, J., Mansour, N.N.: Direct numerical simulation of turbulent channel
731 flow up to $re_\tau=590$. *Physics of Fluids* **11**(4), 943–945 (1999). DOI 10.1063/1.869966
- 732 29. Neves, W., Olivera, C.: Wellposedness for stochastic continuity equations with
733 ladyzhenskaya–prodi–serrin condition. *Nonlinear Differential Equations and Applica-*
734 *tions NoDEA* **22**(5), 1247–1258 (2015). DOI 10.1007/s00030-015-0321-6
- 735 30. Nicoud, F., Ducros, F.: Subgrid-scale stress modelling based on the square of the velocity
736 gradient tensor. *Flow, Turbulence and Combustion* **62**(3), 183–200 (1999). DOI 10.
737 1023/A:1009995426001
- 738 31. Øksendal, B.: *Stochastic Differential Equations*. Springer-Verlag Berlin Heidelberg
739 (2003). DOI 10.1007/978-3-642-14394-6
- 740 32. Oliveira, P.J., Issa, P.I.: An improved piso algorithm for the computation of bouyancy
741 driven flows. *Numerical Heat Transfers, Part B. Fundamentals* **640**, 473 (2001)
- 742 33. Orszag, S.A.: Analytical theories of turbulence. *Journal of Fluid Mechanics* **41**(2),
743 363–386 (1970). DOI 10.1017/S0022112070000642
- 744 34. Piomelli, U.: Large-eddy and direct simulation of turbulent flows. *CFD2001 - 9th*
745 *Conférence Annuelle de la Société Canadienne de CFD* (2001)
- 746 35. Pope, S.: *Turbulent Flows*. Cambridge University Press (2000)
- 747 36. Pope, S.B.: A lagrangian two-time probability density function equation for inhomog-
748 eneous turbulent flows. *The Physics of Fluids* **26**(12), 3448–3450 (1983). DOI
749 10.1063/1.864125

- 750 37. Resseguier, V., Mémin, E., Chapron, B.: Geophysical flows under location uncertainty,
751 Part I: random transport and general models. *Geophysical and Astrophysical Fluid*
752 *Dynamics* **111**(3), 149–176 (2017). DOI 10.1080/03091929.2017.1310210
- 753 38. Resseguier, V., Mémin, E., Chapron, B.: Geophysical flows under location uncertainty,
754 Part II: quasi-geostrophy and efficient ensemble spreading. *Geophysical and Astrophys-*
755 *ical Fluid Dynamics* **111**(3), 177–208 (2017). DOI 10.1080/03091929.2017.1312101
- 756 39. Resseguier, V., Mémin, E., Chapron, B.: Geophysical flows under location uncertainty,
757 Part III: sqg and frontal dynamics under strong turbulence conditions. *Geophysical*
758 *and Astrophysical Fluid Dynamics* **111**(3), 209–227 (2017). DOI 10.1080/03091929.
759 2017.1312102
- 760 40. Resseguier, V., Mémin, E., Heitz, D., Chapron, B.: Stochastic modelling and diffusion
761 modes for proper orthogonal decomposition models and small-scale flow analysis. *Jour-*
762 *nal of Fluid Mechanics* **826**, 888–917 (2017). DOI 10.1017/jfm.2017.467
- 763 41. Roman, F., Stipcich, G., Armenio, V., Inghilesi, R., Corsini, S.: Large eddy simulation
764 of mixing in coastal areas. *International Journal of Heat and Fluid Flow* **31**(3), 327 –
765 341 (2010). DOI doi.org/10.1016/j.ijheatfluidflow.2010.02.006
- 766 42. Sagaut, P.: Large eddy simulation for incompressible flows. An introduction. Springer
767 (2000)
- 768 43. Smagorinsky, J.: General circulation experiments with the primitive equations: I. the
769 basic experiment. *Mon. Weather Rev.* **91**, 99 (1963)
- 770 44. Smith, C.R., Metzler, S.P.: The characteristics of low-speed streaks in the near-wall
771 region of a turbulent boundary layer. *Journal of Fluid Mechanics* **129**, 27–54 (1983).
772 DOI 10.1017/S0022112083000634